Synthesis, crystal structures, and luminescent properties of eleven new lanthanide and yttrium complexes with fluorescent whitener and 1,10-phenanthroline†‡

Ruibiao Fu,* Shengmin Hu, Tianlu Sheng and Xintao Wu*

Received (in Montpellier, France) 10th February 2009, Accepted 25th February 2009
First published as an Advance Article on the web 27th March 2009
DOI: 10.1039/b902803j

Eleven new lanthanide and yttrium complexes: $[M(phen)_2(L)(H_2O)_2]_2\cdot(L)\cdot 2H_2O$ (M = Er (**1**), Dy (**2**), Yb (**3**), Y (**4**), Sm (**5**), Tb (**6**), Ho (**7**), Eu (**8**), Nd (**9**), Tm (**10**), Gd (**11**); L = 4,4′-bis(2-sulfonatostyryl)biphenyl; phen = 1,10-phenanthroline), have been rationally synthesized under hydrothermal conditions and characterized by single-crystal X-ray diffraction together with powder XRD, elemental analyses (EA), IR, thermogravimetric analysis (TGA) and diffuse absorption. Powder XRD patterns of solids **1–11** demonstrate that these compounds are isomorphous. X-Ray single-crystal diffraction reveals that these complexes possess an interesting $[M(phen)_2(L)(H_2O)_2]_2^{2+}$ dimer, which is arranged further to form a 3D structure through hydrogen bonds. Solids **1–11** exhibit attractive photoluminescence due to the **L** anions lying in two different environments. Especially, the luminescent color of solids **2–8** and the lifetime of solid **6** can be reversibly tuned by shifting the wavelength of excited light.

Introduction

Metal–ligand complexes have attracted attention in recent years due to their interesting structures and properties, such as gas adsorption and storage, catalysis, electrical conductivity, non-linear optics, magnetism and so on.[1–4] In particular, the design and synthesis of luminescent metal–ligand complexes has been extensively explored due to their high thermal stability, strong emission and tunable colors, as well as their potential application as light-emitting diodes (LEDs), chemosensors, probes and sensors.[5–8] Recently, we have developed an effective method to synthesize bright luminescent materials by the combination of fluorescent whitener (**Na_2L**) and transition metals through electrostatic interactions, coordination bonds, hydrogen bonds and π–π stacking interactions.[9] These solids display blue–green, green and dark red emissions, which show bathochromic-shifts compared to the blue luminescence of fluorescent whitener. On the other hand, lanthanide complexes with organic ligands are of current research interest for their excellent luminescence, which is attributed to f–f transitions of lanthanide ions with a narrow bandwidth.[10] Looking at the above results, we suggest that the combination of fluorescent whitener and lanthanide would lead to some interesting luminescent materials. Furthermore, 1,10-phenanthroline (denoted as phen) has been selected as a second ligand for lanthanide ions to form Ln–phen cationic fragments, improving the solubility of lanthanide–ligand complexes to grow suitable single crystals.[11] We have successfully obtained ten lanthanide complexes as well as one yttrium isomorph with phen and fluorescent whitener as co-ligands: **$[M(phen)_2(L)(H_2O)_2]_2\cdot(L)\cdot 2H_2O$** (M = Er (**1**), Dy (**2**), Yb (**3**), Y (**4**), Sm (**5**), Tb (**6**), Ho (**7**), Eu (**8**), Nd (**9**), Tm (**10**), Gd (**11**); L = 4,4′-bis(2-sulfonatostyryl)biphenyl). Solids **1–11** exhibit attractive photoluminescence due to the **L** anions lying in two different environments. Especially, the luminescent color of solids **2–8** and the lifetime of solid **6** can be reversibly tuned by shifting the wavelength of excited light.

Results and discussion

Synthesis and characterization

Solids **1–11** were prepared by reaction of $M(ClO_4)_3$, **Na_2L** and 1,10-phenanthroline·H_2O under hydrothermal conditions, and satisfactorily characterized with powder XRD, IR and elemental analyses (EA). Experimental powder XRD patterns of solids **1–11** are all consistent with that simulated from single-crystal X-ray data of compound **1**, which indicates these compounds are isomorphous (Fig. 1). As shown in Fig. S1,‡ solids **1–11** display identical IR spectra. Furthermore, elemental analyses of these compounds are in accord with respective calculated values. These results suggest that the final products of compounds **1–11** are in the homogeneous phase, respectively. The bands centered at 3615 and 3250 cm^{-1} are attributed to the O–H stretching vibration of the isolated and the coordinated water molecules, respectively.

State Key Laboratory of Structural Chemistry, Fujian Institute of Research on the Structure of Matter, Chinese Academy of Science, Fuzhou, Fujian, 350002 China. E-mail: wxt@fjirsm.ac.cn; Fax: +86-591-83794946; Tel: +86-591-83792837

† Dedicated to Prof. Xin-Tao Wu on the occasion of his 70th birthday.

‡ Electronic supplementary information (ESI) available: An X-ray crystallographic information file (CIF) is available for compound **1**. CCDC reference number 679075. IR spectra of **1–11**, TGA curve, powder XRD patterns, diffuse absorbance and ESI mass spectrum of compound **8**, luminescent emission spectra for phenanthroline·H_2O, as well as fluorescence intensity as a function of time for **1–2** and **4–11**. For ESI and crystallographic data in CIF or other electronic format see DOI: 10.1039/b902803j

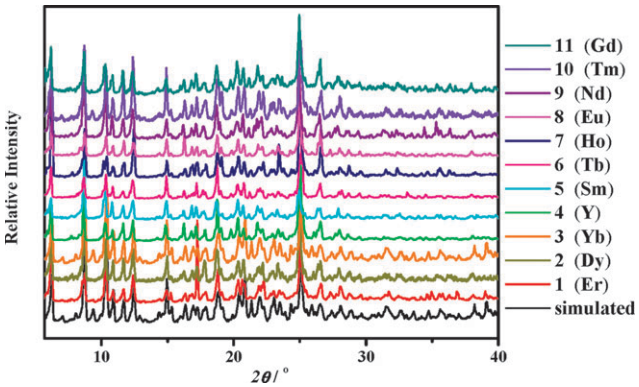

Fig. 1 Powder XRD patterns simulated from single-crystal X-ray data of compound **1** and experimental data for solids **1–11**.

Due to solids **1–11** being isomorphous, only compound **8** (Eu) was selected as an example to investigate the solubility, thermal stability and UV–vis absorption. Compound **8** is insoluble in water, ethanol, acetone and acetonitrile. However, when compound **8** dissolves in dimethyl sulfoxide (DMSO), the $[Eu(phen)_2(L)(H_2O)_2]_2^{2+}$ (m/z = 1064.96) dimer can not be found in the ESI mass spectrum (Fig. S2‡). This indicates that the structure has been dissociated. The thermogravimetric analysis (TGA) curve of compound **8** shows an initial step between 100 and 200 °C, with 4.36% weight loss, corresponding to the loss of the isolated and the coordinated water molecules (calculated 4.03%). A slow step followed by an abrupt weight loss stage then appears from 280 °C, resulting from the decomposition of the phen and the **L** anion. The powder XRD pattern of the dehydrated solid **8**, which has been previously heated at 250 °C under an air atmosphere for two hours and then cooled to room temperature, is different from that of the as-prepared solid. This indicates that the structure has been changed after the loss of three water molecules. The water molecules could not be recovered after the dehydrated solid was exposed to water vapor for 11 days. As shown in Fig. S5,‡ the UV–vis diffuse absorption spectrum of compound **8** reveals that the solid can absorb ultraviolet radiation with a broad band in the range of 200–400 nm.

Structural descriptions

Powder XRD patterns reveal that solids **1–11** are isomorphous. Therefore, only the structure of compound **1** has been characterized by single-crystal X-ray diffraction and described in detail as a representative example. As shown in Fig. 2, compound **1** includes a $[Er(phen)_2(L)(H_2O)_2]_2^{2+}$ dimer, one non-coordinated **L** moiety and two isolated water molecules. The dimer lies about an inversion centre and the non-coordinated **L** moiety also lies about another independent inversion centre. The existences of the isolated and the coordinated water molecules are in accordance with the IR result. The central Er^{3+} ion is coordinated by four nitrogen donors from two bidentate phens, two sulfonate oxygen atoms from two coordinated **L** groups, and two water molecules, resulting in a coordination number of eight. The coordination geometry of the central Er^{3+} ion may be best described as a distorted square antiprism with four oxygen atoms and four nitrogen donors. The bond lengths of Er–N and Er–O are in

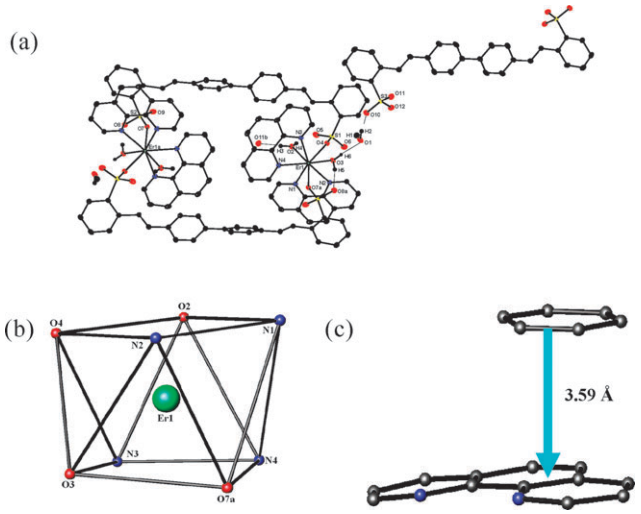

Fig. 2 (a) ORTEP view of the coordination geometries of erbium and sulfur of **1** (ellipsoid at 10% probability). Dotted lines represent hydrogen bonds. Symmetry code for the generated atoms: $a - x, -y, -z$; $b - 1 + x, y, z$. (b) Coordination polyhedron of the Er^{3+} ion. (c) View of the π–π stacking interactions between phen and the benzene ring of the coordinated **L** anion.

the ranges of 2.491(3)–2.529(3) Å and 2.275(2)–2.318(3) Å, respectively (Table 1). Except for the coordinated **L** group, there is also an isolated **L** group which does not take part in coordination with the Er^{3+} ion.

The $[Er(phen)_2(L)(H_2O)_2]_2^{2+}$ dimer consists of two $[Er(phen)_2]^{3+}$ cationic fragments which are bridged by the coordinated **L** groups. In the dimer, there is a 42-membered ring with about 14.9 × 6.7 Å dimensions (calculated from the distance of neighboring S atoms). The coordinated **L** group connects the $[Er(phen)_2]^{3+}$ cationic fragment through two coordination bonds (Er1–O4 and Er–O7), an offset

Table 1 Selected bond lengths (Å) and angles (°) for **1**

Er(1)–N(1)	2.529(3)	S(1)–O(6)	1.440(3)
Er(1)–N(2)	2.517(3)	S(1)–C(25)	1.783(4)
Er(1)–N(3)	2.491(3)	S(2)–O(7)	1.483(2)
Er(1)–N(4)	2.522(3)	S(2)–O(8)	1.450(3)
Er(1)–O(2)	2.318(3)	S(2)–O(9)	1.434(3)
Er(1)–O(3)	2.306(3)	S(2)–C(52)	1.774(4)
Er(1)–O(4)	2.308(2)	S(3)–O(10)	1.450(3)
Er(1)–O(7)[a]	2.275(2)	S(3)–O(11)	1.453(3)
S(1)–O(4)	1.481(3)	S(3)–O(12)	1.432(3)
S(1)–O(5)	1.450(3)	S(3)–C(53)	1.777(4)
N(1)–Er(1)–N(2)	65.02(9)	N(3)–Er(1)–O(2)	77.40(11)
N(1)–Er(1)–N(3)	141.07(10)	N(3)–Er(1)–O(3)	76.22(10)
N(1)–Er(1)–N(4)	82.30(10)	N(3)–Er(1)–O(4)	82.19(10)
N(1)–Er(1)–O(2)	74.77(10)	N(3)–Er(1)–O(7)[a]	107.54(10)
N(1)–Er(1)–O(3)	140.95(10)	N(4)–Er(1)–O(2)	77.61(11)
N(1)–Er(1)–O(4)	114.97(9)	N(4)–Er(1)–O(3)	117.08(11)
N(1)–Er(1)–O(7)[a]	80.84(9)	N(4)–Er(1)–O(4)	140.83(9)
N(2)–Er(1)–N(3)	153.36(10)	N(4)–Er(1)–O(7)[a]	72.35(9)
N(2)–Er(1)–N(4)	138.43(10)	O(2)–Er(1)–O(3)	139.63(11)
N(2)–Er(1)–O(2)	114.70(12)	O(2)–Er(1)–O(4)	74.13(10)
N(2)–Er(1)–O(3)	80.23(10)	O(2)–Er(1)–O(7)[a]	143.39(10)
N(2)–Er(1)–O(4)	78.96(9)	O(3)–Er(1)–O(4)	72.46(10)
N(2)–Er(1)–O(7)[a]	77.46(9)	O(3)–Er(1)–O(7)[a]	74.45(10)
N(3)–Er(1)–N(4)	65.44(10)	O(4)–Er(1)–O(7)[a]	141.97(9)

[a] Symmetry codes: $-x, -y, -z$.

Table 2 Hydrogen bond lengths (Å) and angles (°) for **1**

D–H···A	D–H	H···A	D···A	D–H···A
O1–H2···O10	0.88(7)	1.83(7)	2.711(6)	176(6)
O2–H4···O5	0.70(5)	2.06(6)	2.727(5)	160(6)
O2–H3···O11[b]	0.89(6)	1.75(6)	2.633(4)	173(6)
O3–H6···O1	0.76(5)	1.90(5)	2.658(5)	172(5)
O3–H5···O8[a]	0.83(6)	1.84(6)	2.661(4)	169(5)

[a] Symmetry code: $-x, -y, -z$. [b] Symmetry code: $x - 1, y, z$.

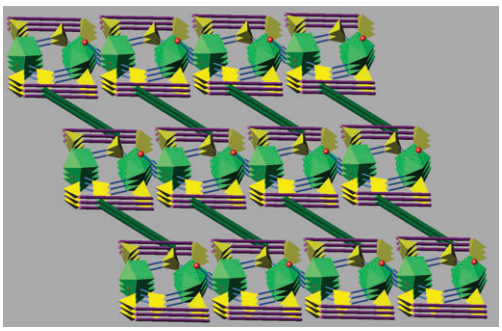

Fig. 3 Polyhedral view of the structure of **1**. $[ErN_4O_4]$ and $[CSO_3]$ are indicated by a green square antiprism and a tetrahedron, respectively. Blue lines: hydrogen bonds; purple lines: the coordinated **L** group; green lines: the isolated **L** group.

face-to-face π–π stacking interaction with adjacent phen groups at a separated distance of 3.59 Å, as well as two hydrogen bonds between a sulfonate oxygen atom and the coordinated water molecules (O2···O5 and O3···O8) (Table 2). The coordinated **L** group displays in a torsional mode with both terminal SO_3 groups lying on the same side. The dihedral angle between the two middle benzene rings is about 41.7°. The mode is similar to that of $[Cd(4,4'\text{-bipy})(L)(H_2O)_2]$.[9c] While the non-coordinated **L** group is in a centrosymmetric mode with two terminal SO_3 groups located at opposite sides of the organic group, which has appeared in $[Co(4,4'\text{-bipy})_2(L)]\cdot 2H_2O$ and $[Co(4,4'\text{-bipy})_2(H_2O)_2](4,4'\text{-bipy})(L)\cdot 2H_2O$.[9c] The non-coordinated **L** group contacts the cationic unit through a hydrogen bond (O2···O11) between a sulfonate oxygen atom (O11) and the coordinated water molecule (O2). In addition, the isolated water molecule adopts a bridging mode to join the non-coordinated **L** group and the dimer through two hydrogen bonds (O1···O3 and O1···O10). All these hydrogen bonds link the dimers, non-coordinated **L** groups and isolated water molecules into a 3D structure (Fig. 3).

Luminescent properties

Solid-state luminescent properties of solids **1–11** were investigated under ambient temperature. The fluorescent data are summarized in Table 3. And the emission spectra are shown in Fig. 4 and 5. As expected, these compounds exhibit attractive photoluminescence. Solid **1** displays a blue–green luminescence with a broad emission spectrum containing two erbium absorption peaks at 487 and 522 nm. The peak emission shows a 30 nm blue-shift by shifting the excited wavelength from 380 to 436 nm. For solid **2**, the blue emission can be easily transformed into blue–green light by shifting the

Table 3 Fluorescent data for solids **1–11**

Complex	Excited/nm	Maximum emission/nm	Lifetime/ns, excited/emission/nm
1	380	513	5.9 ± 3, 370/510
	436	483	
2	355	456	0.88 ± 3, 370/456
	434	494	
3	372	468	
	435	539	
4	377	457	4.5 ± 2, 370/470
	434	485	
5	373	458	7.1 ± 7, 373/537
	450	527	
6	370	451	0.74 ± 2, 370/470
	450	539	12.3 ± 5, 370/550
7	370	464	10.6 ± 4, 370/555
	447	529	
8	377	460	4.1 ± 1, 370/610
	477	588	
Dehydrated **8**	375	565	
9	273	456	1.7 ± 2, 273/456
	338	456	
10	350	519	28.0 ± 2, 370/520
	433	519	
11	380	529	6.5 ± 3, 430/530

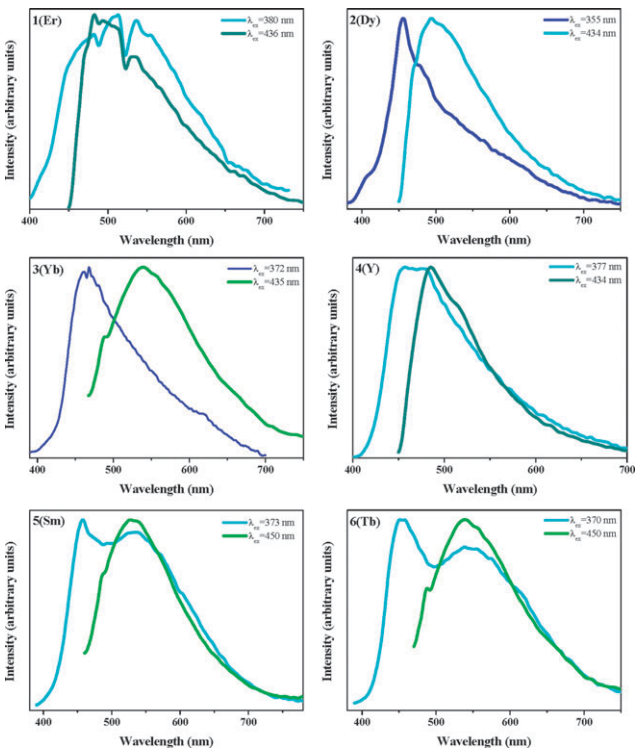

Fig. 4 Normalized solid-state emission spectra for **1–6**.

excited band from 380 to 434 nm. Solid **3** also shows tunable luminescent emission between blue and green light. By shifting the excited band from 377 to 434 nm, the peak band for solid **4** shows a 28 nm red-shift which is different from that of solid **1**. For solids **5–7**, the luminescent color can be tuned between blue–green and green. In addition, the emission profile of compound **7** contains some self-absorption bands due to the Ho^{3+} ion, which is similar to that of compound **1**. And the lifetime of blue emission for solid **6** is about one sixteenth of

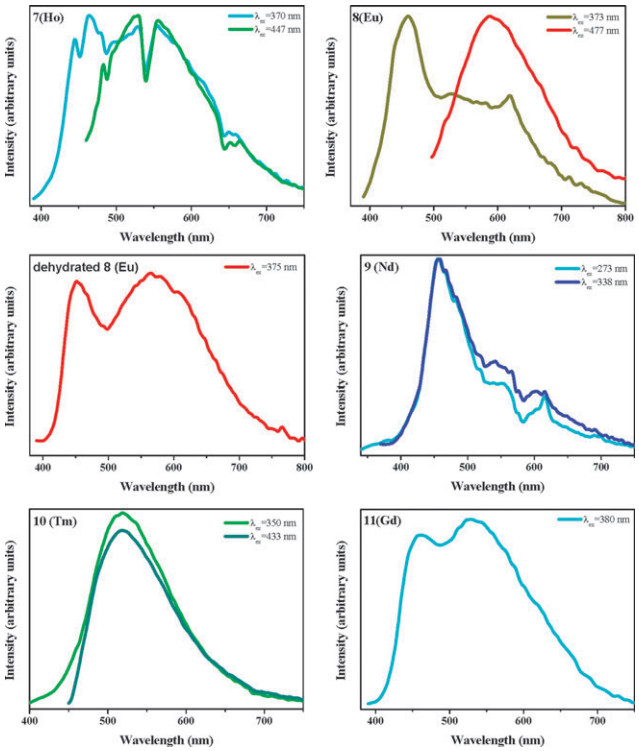

Fig. 5 Normalized solid-state emission spectra for **7–11** and the dehydrated solid **8**.

that of green emission, indicating that the luminescent lifetime for compound **6** can also be easily tuned by shifting the wavelength of excited light.

Solid **8** displays tunable luminescent emission between orange and red. As a result, the maximum band of red emission shows a 168 nm red-shift compared to that of orange light. While the dehydrated solid **8**, which was previously heated at 250 °C under an air atmosphere for two hours and then cooled to room temperature, displays red luminescence when excited by a hand-held UV lamp with an excitation wavelength of 365 or 254 nm. The saddle-like emission profile is different from that of as-prepared solid **8**. This is because the structure has been changed after being dehydrated. In addition, after solid **8** dissolves in DMSO, the solution can give off bright purple–blue luminescence when excited by a hand-held UV lamp with an excitation wavelength of 365 or 254 nm, which is different behaviour to that of solid **8**. However, the emission is the same as that of **Na_2L**–DMSO solution, indicating that the structure of solid **8** dissociates after dissolving in DMSO. This result is in accordance with the ESI mass spectrum.‡

Solids **9–11** display blue, green and blue–green emission, respectively. The emission profile of solid **9** is narrow, which is different from those of solids **1** and **5–8**. This is attributed to the Nd^{3+} ion absorbing the green and yellow light around 526 and 584 nm, respectively. While the broad saddle-like emission profile of compound **11** is similar to those of solids **5–7**.

The spectra of lanthanide ion luminescence usually exhibit long lifetime and sharp emission features due to f–f transitions, which neglect environmental influences since the 4f electrons are shielded by filled 5s and 5p orbitals.[10h,11a,12] In contrast, the luminescence of these complexes displays a broad profile and short lifetime. So the emissions of these compounds may not be attributed to the lanthanide centers. And since 1,10-phenanthroline·H_2O shows weak purple (λ_{max} = 419 nm, excited at 370 nm) or ultraviolet (λ_{max} = 381 nm, excited at 342 nm) emissions with narrow profiles, the emissions of these compounds cannot be assigned to the ligand-centered π–π* transition of the phen group. On one hand, the bright blue–green emission of $[Zn_2(Im)_2(ImH)_4](L)$ originates from the ligand-centered π–π* transition of the isolated **L** group, since **Na_2L** can also emit a similar emission with a maximum band at 452 nm.[9c] And in the structure of $[Zn_2(Im)_2(ImH)_4](L)$, the **L** anion does not take part in coordination, nor contact with the adjacent organic moiety through π–π stacking interactions. This is similar to the isolated **L** anion in the structures of solids **1–11**. With excitation by ultraviolet radiation, the luminescence profiles in the blue region for solids **1–9** and **11** show maximum bands in the range of 451–468 nm, which are close to those of **Na_2L** and $[Zn_2(Im)_2(ImH)_4](L)$. Furthermore, the lifetime of blue emission for solids **2** and **6** match well with that of $[Zn_2(Im)_2(ImH)_4](L)$. The above results indicate the luminescent emission in the blue region for solids **1–9** and **11** mainly originates from the ligand-centered π–π* transition of the isolated **L** group. On the other hand, in the structures of $[Cd(4,4'\text{-bipy})(L)(H_2O)_2]$ and $[Zn(4,4'\text{-bipy})(H_2O)_4]$-$[Zn(4,4'\text{-bipy})_{1.5}(L)(H_2O)_2]_2(L)\cdot 6H_2O$, the **L** anion makes contact with the adjacent organic moiety through π–π stacking interactions, resulting in the emissions exhibiting about 18 and 90 nm bathochromic-shifts compared to that of **Na_2L**, respectively.[9b,c] Similarly, the coordinated **L** anion in solids **1–11** also contacts with the adjacent phen group through a π–π stacking interaction. So for solids **1–11**, the luminescent emission in the green region may be assigned to the ligand-centered π–π* transition of the coordinated **L** group.

In addition, no near-infrared (NIR) fluorescent emissions for these compounds were observed, though NIR luminescence of Nd^{3+}, Er^{3+} and Yb^{3+} ions can be achieved with suitable ligands.[10j,13] This indicates that in the structures of solids **1–11**, phen and **L** cannot sensitize the NIR luminescence of lanthanide ions.

Conclusions

In summary, a series of new lanthanide and yttrium complexes containing fluorescent whitener and phen have been successfully synthesized, and the systematic synthetic procedure has been well established. These solids possess an interesting dimer, which is further linked by the isolated water molecules and **L** anion groups through hydrogen bonds into 3D structures. Although the luminescence of lanthanide ions is not sensitized by a phen group and an **L** anion, solids **1–11** exhibit attractive fluorescence due to the **L** anions lying in two different environments. Especially, the luminescent color of solids **2–8** and the lifetime of solid **6** can be easily tuned by shifting the wavelength of excited light. This provides a rational synthetic strategy for the construction of intriguing photoluminescent materials. Future research will be focused on the preparation of new lanthanide complexes with different

ratios of reactants to investigate the relationship between luminescent property and structure.

Experimental

Materials and instrumentation

All chemicals were obtained from commercial sources without further purification. 0.5 M $M(ClO_4)_3$ solutions were prepared by dissolving lanthanide oxide in excess perchloric acid. These compounds were synthesized in 25 ml Teflon-lined stainless steel vessels under autogenous pressure. The reactants were stirred homogeneously before heating. Elemental analyses were carried out with a Vario EL III element analyzer. Infrared spectra were obtained on a Nicolet Magna 750 FT-IR spectrometer. Photoluminescence analyses for these solids were performed with Edinburgh FLS920 and LifeSpec-ps fluorescence spectrometers. The diffuse absorption spectrum and the ESI mass spectrum of compound **8** were recorded on a Perkin-Elmer Lambda 900 UV-VIS-NIR spectrometer and DECAX-30000 LCQ Deca XP spectrometer, respectively. Thermogravimetric analysis (TGA) was performed on a NETZSCH STA449C under nitrogen gas flow at a heating rate of 10 °C min^{-1} from room temperature to 1000 °C. Powder X-ray diffraction (XRD) patterns were acquired on a DMAX-2500 diffractometer using Cu Kα radiation under ambient conditions.

Synthesis of the complexes

$[Er(phen)_2(L)(H_2O)_2]_2\cdot(L)\cdot 2H_2O$ (1). A mixture of 0.5 M $Er(ClO_4)_3$ (0.2 ml, 0.1 mmol), **Na_2L** (0.0850 g, 0.1511 mmol), 1,10-phenanthroline·H_2O (0.0364 g, 0.184 mmol) and H_2O (10.0 ml, 556 mmol) was heated at 120 °C for 96 h. After the mixture was cooled slowly to ambient temperature, yellow–green prismatic crystals were obtained. The final pH of the solution was 4.97. The crystals were filtered, washed with distilled water and dried at ambient temperature. A suitable crystal was selected for single crystal X-ray diffraction studies. The experimental powder XRD pattern was in accordance with that simulated from single-crystal X-ray data, which indicated the homogenous phase of the product. The yield was 24% (0.0301 g) based on 1,10-phenanthroline·H_2O. Anal. calc. for $C_{132}H_{104}N_8O_{24}S_6Er_2$ **1**: C 58.43, H 3.86, N 4.13%. Found: C 57.81, H 4.02, N 3.65%. IR (KBr pellet, cm^{-1}): 3617m, 3251m, 3062m, 3026m, 1627m, 1589m, 1521m, 1495m, 1464m, 1426s, 1344w, 1302w, 1252s, 1226s, 1211s, 1168s, 1155s, 1132s, 1106w, 1079s, 1043w, 1016s, 965m, 860m, 846m, 808m, 763m, 754m, 744w, 730m, 725m, 697m, 639m, 613m, 595w, 578w, 561w, 539w.

$[Dy(phen)_2(L)(H_2O)_2]_2\cdot(L)\cdot 2H_2O\cdot$(2). A mixture of 0.5 M $Dy(ClO_4)_3$ (0.4 ml, 0.2 mmol), **Na_2L** (0.1736 g, 0.3086 mmol), 2 M NaOH (0.05 ml, 0.1 mmol), 1,10-phenanthroline·H_2O (0.0742 g, 0.374 mmol) and H_2O (10.0 ml, 556 mmol) was heated at 180 °C for 120 h. After the mixture was cooled slowly to ambient temperature, yellow–green prismatic crystals were obtained. The final pH of the solution was 6.0. The experimental powder XRD pattern was in agreement with that simulated from single-crystal X-ray data of **1**, which indicated the homogenous phase of the product. The yield was 81% (0.2044 g) based on 1,10-phenanthroline·H_2O. Anal. calc. for $C_{132}H_{104}N_8O_{24}S_6Dy_2$ **2**: C 57.87, H 3.97, N 4.09%. Found: C 57.33, H 3.91, N 3.81%. IR (KBr pellet, cm^{-1}): 3612m, 3263m, 3062m, 3026m, 1626m, 1589m, 1520m, 1495m, 1464m, 1426m, 1344w, 1252s, 1227s, 1209s, 1168s, 1152s, 1132s, 1104w, 1079s, 1044w, 1016s, 1004m, 964m, 860m, 845m, 808m, 762m, 754m, 730m, 724w, 697m, 638m, 613s, 595m, 578m, 561m, 539m.

$[Yb(phen)_2(L)(H_2O)_2]_2\cdot(L)\cdot 2H_2O$ (3). A mixture of Yb_2O_3 (0.0394 g, 0.100 mmol), perchloric acid (0.12 ml, 2.1 mmol) and H_2O (10.0 ml, 556 mmol) was previously heated at 150 °C for 20 h. After being cooled to room temperature, **Na_2L** (0.1736 g, 0.3086 mmol) and 1,10-phenanthroline·H_2O (0.0741 g, 0.374 mmol) were added and then heated at 120 °C for 96 h. After the mixture was cooled slowly to ambient temperature, yellow–green prismatic crystals were obtained. The final pH of the solution was 3.00. The experimental powder XRD pattern was in agreement with that simulated from single-crystal X-ray data of **1**, which indicated the homogenous phase of the product. The yield was 43% (0.1103 g) based on 1,10-phenanthroline·H_2O. Anal. calc. for $C_{132}H_{104}N_8O_{24}S_6Yb_2$ **3**: C 58.19, H 3.85, N 4.11%. Found: C 57.40, H 3.74, N 3.92%. IR (KBr pellet, cm^{-1}): 3618m, 3241m, 3062m, 3026w, 3007w, 1628m, 1589m, 1495m, 1464m, 1425m, 1344w, 1252s, 1226m, 1211m, 1168s, 1155s, 1132m, 1106w, 1080s, 1043w, 1016s, 964m, 860m, 846m, 808m, 763m, 754m, 731m, 697m, 640m, 613s, 596m, 578m, 561m, 539m.

$[Y(phen)_2(L)(H_2O)_2]_2\cdot(L)\cdot 2H_2O$ (4). Compound **4** was synthesized by the same procedure as **1** except for the replacement of $Er(ClO_4)_3$ with $Y(ClO_4)_3$. The final pH of the solution was 4.95. The experimental powder XRD pattern was in agreement with that simulated from single-crystal X-ray data of **1**, which indicated the homogenous phase of the product. The yield was 43% (0.0509 g) based on 1,10-phenanthroline·H_2O. Anal. calc. for $C_{132}H_{104}N_8O_{24}S_6Y_2$ **4**: C 62.02, H 4.10, N 4.38%. Found: C 61.56, H 3.96, N 4.12%. IR (KBr pellet, cm^{-1}): 3617m, 3254m, 3062m, 3026m, 1627m, 1589m, 1521m, 1495m, 1464m, 1426s, 1344w, 1302w, 1252s, 1226s, 1211s, 1168s, 1156s, 1132s, 1106w, 1079s, 1044w, 1016s, 965m, 860m, 846m, 808m, 762m, 754m, 744w, 730m, 725m, 697m, 639m, 613m, 595w, 578w, 561w, 539w.

$[Sm(phen)_2(L)(H_2O)_2]_2\cdot(L)\cdot 2H_2O$ (5). A mixture of 0.5 M $Sm(ClO_4)_3$ (0.4 ml, 0.2 mmol), **Na_2L** (0.1700 g, 0.3022 mmol), 1,10-phenanthroline·H_2O (0.0730 g, 0.368 mmol) and H_2O (10.0 ml, 556 mmol) was heated at 120 °C for 96 h. After the mixture was cooled slowly to ambient temperature, yellow–green prismatic crystals were obtained. The final pH of the solution was 5.44. The experimental powder XRD pattern was in agreement with that simulated from single-crystal X-ray data of **1**, which indicated the homogenous phase of the product. The yield was 72% (0.1773 g) based on 1,10-phenanthroline·H_2O. Anal. calc. for $C_{132}H_{104}N_8O_{24}S_6Sm_2$ **5**: C 59.17, H 3.91, N 4.18%. Found: C 58.72, H 3.71, N 3.90%. IR (KBr pellet, cm^{-1}): 3614m, 3259m, 3061m, 3026m, 1625m, 1589m, 1520m, 1495m, 1464m, 1426s, 1343w, 1302w, 1252s, 1226s, 1209s, 1168s, 1152s, 1132s, 1104w, 1079s, 1044w, 1016s, 1004m, 964m, 860m, 845m, 808m, 762m, 753m,

744w, 730m, 724m, 697m, 638m, 613s, 595m, 578w, 560w, 538w.

[Tb(phen)$_2$(L)(H$_2$O)$_2$]$_2$·(L)·2H$_2$O (6). Compound **6** was synthesized by the same procedure as **1** except for the replacement of Er(ClO$_4$)$_3$ with Tb(ClO$_4$)$_3$. The final pH of the solution was 3.50. The yield was 70% (0.0867 g) based on 1,10-phenanthroline·H$_2$O. The experimental powder XRD pattern was in agreement with that simulated from single-crystal X-ray data of **1**, which indicated the homogenous phase of the product. Anal. calc. for C$_{132}$H$_{104}$N$_8$O$_{24}$S$_6$Tb$_2$ **6**: C 58.80, H 3.89, N 4.16%. Found: C 58.52, H 3.7, N 3.91%. IR (KBr pellet, cm^{-1}): 3616m, 3251m, 3061m, 3026m, 3006w, 1626m, 1589m, 1578w, 1520m, 1494m, 1464m, 1426s, 1344w, 1302w, 1252s, 1226s, 1209s, 1168s, 1152s, 1132s, 1105w, 1079s, 1044w, 1016s, 1006s, 964m, 860m, 845m, 808m, 762m, 753m, 744w, 730m, 724m, 697m, 638m, 613s, 595w, 578m, 560m, 538m.

[Ho(phen)$_2$(L)(H$_2$O)$_2$]$_2$·(L)·2H$_2$O (7). Compound **7** was synthesized by the same procedure as **5** except for the replacement of Sm(ClO$_4$)$_3$ with Ho(ClO$_4$)$_3$. The final pH of the solution was 2.59. The experimental powder XRD pattern was in agreement with that simulated from single-crystal X-ray data of **1**, which indicated the homogenous phase of the product. The yield was 33% (0.0819 g) based on 1,10-phenanthroline·H$_2$O. Anal. calc. for C$_{132}$H$_{104}$N$_8$O$_{24}$S$_6$Ho$_2$ **7**: C 58.54, H 3.87, N 4.14%. Found: C 58.19, H 3.69, N 3.87%. IR (KBr pellet, cm^{-1}): 3617m, 3255m, 3062m, 3026w, 1626m, 1589m, 1578w, 1521m, 1494m, 1463m, 1426s, 1344w, 1252s, 1226s, 1210s, 1168s, 1155s, 1132s, 1106w, 1079s, 1043w, 1016s, 1009m, 964m, 860m, 846m, 808m, 762m, 753m, 730m, 725w, 697m, 639m, 612s, 595m, 578m, 560m, 538m.

[Eu(phen)$_2$(L)(H$_2$O)$_2$]$_2$·(L)·2H$_2$O (8). A mixture of 0.5 M Eu(ClO$_4$)$_3$ (0.4 ml, 0.2 mmol), **Na$_2$L** (0.1736 g, 0.3086 mmol), 2 M NaOH (0.1 ml, 0.2 mmol), 1,10-phenanthroline·H$_2$O (0.0741 g, 0.374 mmol) and H$_2$O (10.0 ml, 556 mmol) was heated at 160 °C for 120 h. After the mixture was cooled slowly to ambient temperature, yellow–green prismatic crystals were obtained. The final pH of the solution was 4.50. The experimental powder XRD pattern was in agreement with that simulated from single-crystal X-ray data of **1**, which indicated the homogenous phase of the product. The yield was 48% (0.1201 g) based on 1,10-phenanthroline·H$_2$O. Anal. calc. for C$_{132}$H$_{104}$N$_8$O$_{24}$S$_6$Eu$_2$ **8**: C 59.10, H 3.91, N 4.18%. Found: C 58.65, H 3.71, N 3.97%. IR (KBr pellet, cm^{-1}): 3613m, 3253m, 3061m, 3026m, 1625m, 1589m, 1520m, 1495m, 1464m, 1426s, 1343w, 1252s, 1226s, 1209s, 1168s, 1152s, 1132s, 1105w, 1078s, 1044w, 1016s, 1005m, 964m, 860m, 845m, 808m, 762m, 753m, 730m, 724w, 697m, 638m, 613s, 595m, 578m, 560m, 538m. Compound **8** can also be obtained under high temperature as follows. A mixture of 0.5 M Eu(ClO$_4$)$_3$ (0.4 ml, 0.2 mmol), **Na$_2$L** (0.1736 g, 0.3086 mmol), 2 M NaOH (0.1 ml, 0.2 mmol), 1,10-phenanthroline·H$_2$O (0.0742 g, 0.374 mmol) and H$_2$O (10.0 ml, 556 mmol) was heated at 180 °C for 120 h. After the mixture was cooled slowly to ambient temperature, yellow–green prismatic crystals were obtained. The final pH of the solution was 2.74. The experimental powder XRD pattern was in agreement with that simulated from single-crystal X-ray data of **1**, which indicated the homogenous phase of the product. The yield was 49% (0.1226 g) based on 1,10-phenanthroline·H$_2$O. Compound **8** can also be prepared under low temperature as follows. A mixture of Eu$_2$O$_3$ (0.0364 g, 0.103 mmol), perchloric acid (0.08 ml, 1.4 mmol) and H$_2$O (10.0 ml, 556 mmol) was previously heated at 150 °C for 20 h. After being cooled to room temperature, **Na$_2$L** (0.1736 g, 0.3086 mmol) and 1,10-phenanthroline·H$_2$O (0.0741 g, 0.3738 mmol) were added and then heated at 120 °C for 96 h. After the mixture was cooled slowly to ambient temperature, yellow–green prismatic crystals were obtained. The final pH of the solution was 3.82. The experimental powder XRD pattern was in agreement with that simulated from single-crystal X-ray data of **1**, which indicated the homogenous phase of the product. The yield was 74% (0.1862 g) based on 1,10-phenanthroline·H$_2$O.

[Nd(phen)$_2$(L)(H$_2$O)$_2$]$_2$·(L)·2H$_2$O (9). The synthesis procedure for compound **9** was almost the same as that of **1** except that Nd(ClO$_4$)$_3$ and 2 M NaOH (0.1 ml, 0.2 mmol) were used. The final pH of the solution was 4.85. The experimental powder XRD pattern was in agreement with that simulated from single-crystal X-ray data of **1**, which indicated the homogenous phase of the product. The yield was 65% (0.0800 g) based on 1,10-phenanthroline·H$_2$O. Anal. calc. for C$_{132}$H$_{104}$N$_8$O$_{24}$S$_6$Nd$_2$ **9**: C 59.44, H 3.93, N 4.20%. Found: C 58.59, H 4.47, N 3.97%. IR (KBr pellet, cm^{-1}): 3614m, 3261m, 3062m, 3025m, 1625m, 1589m, 1578w, 1519m, 1494m, 1464m, 1426s, 1343w, 1302w, 1251s, 1226s, 1208m, 1168s, 1151s, 1132s, 1103w, 1078s, 1044w, 1016s, 1002s, 964m, 860m, 846m, 808m, 762m, 753m, 729m, 723m, 696m, 638m, 612m, 595m, 577w, 560w, 538w.

[Tm(phen)$_2$(L)(H$_2$O)$_2$]$_2$·(L)·2H$_2$O (10). The synthesis procedure for compound **10** was almost the same as that of **2** except that Tm(ClO$_4$)$_3$ and 2 M NaOH (0.35 ml, 0.7 mmol) were used. The final pH of the solution was 4.70. The experimental powder XRD pattern was in agreement with that simulated from single-crystal X-ray data of **1**, which indicated the homogenous phase of the product. The yield was 46% (0.1180 g) based on 1,10-phenanthroline·H$_2$O. Anal. calc. for C$_{132}$H$_{104}$N$_8$O$_{24}$S$_6$Tm$_2$ **10**: C 57.60, H 3.95, N 4.07%. Found: C 57.29, H 3.82, N 3.65%. IR (KBr pellet, cm^{-1}): 3617m, 3245m, 3062m, 3027m, 1627m, 1589m, 1522m, 1496m, 1465m, 1426m, 1344w, 1252s, 1226s, 1212m, 1168s, 1155s, 1132s, 1106w, 1080s, 1044w, 1016s, 965m, 860m, 846m, 808m, 763m, 754m, 730m, 697m, 640m, 613s, 595m, 578m, 561m, 539 m.

[Gd(phen)$_2$(L)(H$_2$O)$_2$]$_2$·(L)·2H$_2$O (11). Compound **11** was synthesized by the same procedure as **1** except for the replacement of Er(ClO$_4$)$_3$ with Gd(ClO$_4$)$_3$. The final pH of the solution was 3.79. The experimental powder XRD pattern was in agreement with that simulated from single-crystal X-ray data of **1**, which indicated the homogenous phase of the product. The yield was 19% (0.0233 g) based on 1,10-phenanthroline·H$_2$O. Anal. calc. for C$_{132}$H$_{104}$N$_8$O$_{24}$S$_6$Gd$_2$ **11**: C 58.87, H 3.89, N 4.16%. Found: C 58.53, H 3.70, N 3.90%. IR (KBr pellet, cm^{-1}): 3615m, 3259w, 3060m, 3026m, 1626m, 1589m, 1520m, 1495m, 1464m, 1425s, 1344w, 1302w, 1251s, 1226s, 1209s, 1168s, 1154s, 1132s, 1106w, 1078s, 1043w, 1016s,

964m, 860m, 845m, 808m, 762m, 754m, 744w, 729m, 723m, 696m, 638m, 613m, 595w, 578w, 561w, 538w.

X-Ray crystallography

X-Ray data for compound **1** were collected on a Rigaku Mercury CCD/AFC diffractometer using graphite-monochromated Mo Kα radiation (λ(Mo Kα) = 0.71073 Å). Data were reduced with CrystalClear v1.3. The structure was solved by direct methods and refined by full-matrix least-squares techniques on F^2 using SHELXTL-97.[14] All non-hydrogen atoms were treated anisotropically. Hydrogen atoms which bonded to carbon atoms were generated geometrically, while hydrogen atoms of water molecules were generated from difference Fourier maps and with fixed isotropic thermal parameters. Crystal data for **1**: $C_{132}H_{104}N_8O_{24}S_6Er_2$, M_r = 2713.11, triclinic, space group $P\bar{1}$, a = 11.938, b = 15.1750(2), c = 17.5546(2) Å, α = 81.079(6), β = 76.752(6), γ = 69.389(4)°, Z = 1, ρ_{calcd} = 1.560 g cm^{-3}, μ = 1.631 mm^{-1}, F(000) = 1376, GOF = 1.099, T = 293(2) K. A total of 22373 reflections were collected and 13049 are unique (R_{int} = 0.0228), 11842 observed reflections [$I > 2\sigma(I)$] with $R1$ = 0.0397 and w$R2$ = 0.0843; $R1$ = 0.0461 and w$R2$ = 0.0887 (all data). CCDC 679075.‡

References

1 (*a*) C. Janiak, *Dalton Trans*., 2003, 2781; (*b*) N. L. Rosi, J. Kim, M. Eddaoudi, B. Chen, M. O'Keeffe and O. M. Yaghi, *J. Am. Chem. Soc*., 2005, **127**, 1504; (*c*) J. S. Seo, D. Whang, H. Lee, S. I. Jun, J. Oh, Y. J. Jeon and K. Kim, *Nature*, 2000, **404**, 982; (*d*) O. R. Evans and W. Lin, *Acc. Chem. Res*., 2002, **35**, 511; (*e*) R. Jain, K. Kabir, J. B. Gilroy, K. A. R. Mitchell, K. C. Wong and R. G. Hicks, *Nature*, 2007, **445**, 291.

2 (*a*) A. de Bettencourt-Dias, *Dalton Trans*., 2007, 2229; (*b*) C. Serre, C. Mellot-Draznieks, S. Surblé, N. Audebrand, Y. Filinchuk and G. Férey, *Science*, 2007, **315**, 1828; (*c*) J. Hafizovic, M. Bjørgen, U. Olsbye, P. D. C. Dietzel, S. Bordiga, C. Prestipino, C. Lamberti and K. P. Lillerud, *J. Am. Chem. Soc*., 2007, **129**, 3612; (*d*) S. M. Humphrey, J. S. Chang, S. H. Jhung, J. W. Yoon and P. T. Wood, *Angew. Chem., Int. Ed*., 2007, **46**, 272.

3 (*a*) G. A. Molander and J. A. C. Romero, *Chem. Rev*., 2002, **102**, 2161; (*b*) C. Benelli and D. Gatteschi, *Chem. Rev*., 2002, **102**, 2369; (*c*) V. Baskar, M. Shanmugam, E. C. Sañudo, M. Shanmugam, D. Collison, E. J. L. McInnes, Q. Wei and R. E. P. Winpenny, *Chem. Commun*., 2007, 37; (*d*) J. M. Taylor, A. H. Mahmoudkhani and G. K. H. Shimizu, *Angew. Chem., Int. Ed*., 2007, **46**, 795; (*e*) R. B. Fu, X. H. Huang, S. M. Hu, S. C. Xiang and X. T. Wu, *Inorg. Chem*., 2006, **45**, 5254.

4 (*a*) F. Gándara, J. Perles, N. Snejko, M. Iglesias, B. Gómez-Lor, E. Gutiérrez-Puebla and M. Ángeles Monge, *Angew. Chem., Int. Ed*., 2006, **45**, 7998; (*b*) M. Makha, A. N. Sobolev and C. L. Raston, *Chem. Commun*., 2006, 511; (*c*) J. W. Cai, *Coord. Chem. Rev*., 2004, **248**, 1061; (*d*) S. J. Dalgarno and C. L. Raston, *Chem. Commun*., 2002, 2216; (*e*) M. Makha, A. N. Sobolev and C. L. Raston, *Chem. Commun*., 2006, 57.

5 (*a*) J. C. G. Bünzli and C. Piguet, *Chem. Rev*., 2002, **102**, 1897; (*b*) Z. F. Chen, R. G. Xiong, J. Zhang, J. L. Zuo, X. Z. You, C. M. Che and H. K. Fun, *J. Chem. Soc., Dalton Trans*., 2000, 4010; (*c*) J. C. Dai, X. T. Wu, Z. Y. Fu, C. P. Cui, S. M. Hu, W. X. Du, L. M. Wu, H. H. Zhang and R. Q. Sun, *Inorg. Chem*., 2002, **41**, 1391; (*d*) J. C. Dai, X. T. Wu, S. M. Hu, Z. Y. Fu, J. J. Zhang, W. X. Du, H. H. Zhang and R. Q. Sun, *Eur. J. Inorg. Chem*., 2004, 2096; (*e*) B. Paul, B. Zimmermann, K. M. Fromm and C. Janiak, *Z. Anorg. Allg. Chem*., 2004, **630**, 1650.

6 (*a*) J. C. Dai, X. T. Wu, Z. Y. Fu, S. M. Hu, W. X. Du, C. P. Cui, L. M. Wu, H. H. Zhang and R. Q. Sun, *Chem. Commun*., 2002, 12; (*b*) J. Tao, M. L. Tong, J. X. Shi, X. M. Chen and S. W. Ng, *Chem. Commun*., 2000, 2043; (*c*) J. L. Song, H. H. Zhao, J. G. Mao and K. R. Dunbar, *Chem. Mater*., 2004, **16**, 1884.

7 (*a*) J. Zhang, W. Lin, Z. F. Chen, R. G. Xiong, B. F. Abrahams and H. K. Fun, *J. Chem. Soc., Dalton Trans*., 2001, 1806; (*b*) C. D. Wu, H. L. Ngo and W. Lin, *Chem. Commun*., 2004, 1588; (*c*) L. Han, M. C. Hong, R. H. Wang, J. H. Luo, Z. Z. Lin and D. Q. Yuan, *Chem. Commun*., 2003, 2580; (*d*) J. M. Shi, W. Xu, Q. Y. Liu, F. L Liu, Z. L. Huang, H. Lei, W. T. Yu and Q. Fang, *Chem. Commun*., 2002, 756.

8 (*a*) E. Beurer, J. Grimm, P. Gerner and H. U. Güdel, *J. Am. Chem. Soc*., 2006, **128**, 3110; (*b*) M. Royzen, A. Durandin, V. G. Young, Jr, N. E. Geacintov and J. W. Canary, *J. Am. Chem. Soc*., 2006, **128**, 3854; (*c*) Y. G. Ma, C. M. Che, H. Y. Chao, X. M. Zhou, W. H. Chan and J. C. Shen, *Adv. Mater*., 1999, **11**, 852.

9 (*a*) J. M. A. Stoll and W. Giger, *Anal. Chem*., 1997, **69**, 2594; (*b*) R. B. Fu, S. C. Xiang, S. M. Hu, L. S. Wang, Y. M. Li, X. H. Huang and X. T. Wu, *Chem. Commun*., 2005, 5292; (*c*) R. B. Fu, S. M. Hu and X. T. Wu, *Inorg. Chem*., 2007, **46**, 9630.

10 (*a*) J. C. G. Bünzli and C. Piguet, *Chem. Soc. Rev*., 2005, **34**, 1048; (*b*) K. Kuriki and Y. Koike, *Chem. Rev*., 2002, **102**, 2347; (*c*) H. Tsukube and S. Shinoda, *Chem. Rev*., 2002, **102**, 2389; (*d*) B. S. Harrison, T. J. Foley, A. S. Knefely, J. K. Mwaura, G. B. Cunningham, T. S. Kang, M. Bouguettaya, J. M. Boncella, J. R. Reynolds and K. S. Schanze, *Chem. Mater*., 2004, **16**, 2938; (*e*) P. Wang, J. P. Ma, Y. B. Dong and R. Q. Huang, *J. Am. Chem. Soc*., 2007, **129**, 10620; (*f*) Y. B. Dong, P. Wang, J. P. Ma, X. X. Zhao, H. Y. Wang, B. Tang and R. Q. Huang, *J. Am. Chem. Soc*., 2007, **129**, 4872; (*g*) Y. G. Huang, B. L. Wu, D. Q. Yuan, Y. Q. Xu, F. L. Jiang and M. C. Hong, *Inorg. Chem*., 2007, **46**, 1171; (*h*) J. Xia, B. Zhao, H. S. Wang, W. Shi, Y. Ma, H. B. Song, P. Cheng, D. Z. Liao and S. P. Yan, *Inorg. Chem*., 2007, **46**, 3450; (*i*) Y. Q. Sun, J. Zhang and G. Y. Yang, *Chem. Commun*., 2006, 4700; (*j*) L. N. Sun, H. J. Zhang, Q. G. Meng, F. Y. Liu, L. S. Fu, C. Y. Peng, J. B. Yu, G. L. Zheng and S. B. Wang, *J. Phys. Chem. B*, 2005, **109**, 6174; (*k*) S. Biju, D. B. Ambili Raj, M. L. P. Reddy and B. M. Kariuki, *Inorg. Chem*., 2006, **45**, 10651.

11 (*a*) Y. H. Wang, L. P. Zhang, L. P. Jin, S. Gao and S. Z. Lu, *Inorg. Chem*., 2003, **42**, 4985; (*b*) Z. Y. Du, H. B. Xu and J. G. Mao, *Inorg. Chem*., 2006, **45**, 9780.

12 A. Sonnauer, C. Näther, H. A. A. Höppe, J. Senker and N. Stock, *Inorg. Chem*., 2007, **46**, 9968.

13 M. Albrecht, O. Osetska, J. Klankermayer, R. Fröhlich, F. Gumy and J.-C. G. Bünzli, *Chem. Commun*., 2007, 1834.

14 G. M. Sheldrick, *SHELXT 97, Program for Crystal Structure Refinement*, University of Göttingen, Germany, 1997.

